Charlie Waugh   ORCID iD: 0000-0002-3090-046X

The Impact of Mild Hypercholesterolemia on Injury Repair in the Rat Patellar Tendon

Waugh CM[1,2]., Mousavizadeh R[1]., Lee J[1]., Screen HRC[2]., Scott A[1].

[1]Dept. Physical Therapy, Faculty of Medicine, University of British Columbia, Canada

[2]School of Engineering and Materials Science, Queen Mary, University of London, U.K

Corresponding Author: Charlie M. Waugh

Address: Dept. Physical Therapy, 2177 Westbrook Mall, University of British Columbia, Vancouver B.C, Canada

Tel: +1 604 675-2575

Fax: +1 604 875 2576

E-mail: cmwaugh@mail.ubc.ca

Running title: Hypercholesterolemia Impacts Tendon Injury Repair Processes

Author Contributions Statement: Conceptualization (CW, AS, HS), funding acquisition (CW, AS, HS), resources (AS), methodology (CW, AS, HS, RM), investigation (CW, RM, JL), project administration (CW), data curation and analysis (CW, RM), writing and visualization (CW), review and editing (CW, AS, HS, RM).

ABBREVIATIONS

3-hyp, 4-hyp   hydroxyproline residue

ApoE   apolipoprotein

ApoE^{-/-}   ApoE rat knockout model

COL1A1   collagen type I alpha 1 chain

COL3A1   collagen type III alpha 1 chain

COX-2   cyclo-oxygenase-2

ECM   extracellular matrix

FH   familial hypercholesterolemia

IL-1   interleukin-1

LDL   low-density lipoprotein

LOX   Lysyl oxidase

oxLDL   oxidized low-density lipoprotein

PT   patellar tendon

SD   Sprague Dawley

TC   Triglycerides

WT   wild-type

ABSTRACT

Hypercholesterolemia is associated with tendon pathology and injury prevalence. Lipids

can accumulate in the tendon's extracellular spaces, which may disrupt its hierarchical

structure and the tenocytes physicochemical environment. We hypothesized that the

tendon's ability to repair after injury would be attenuated with elevated cholesterol levels, leading to inferior mechanical properties.

50 wild-type (SD) and 50 apolipoprotein E knock-out rats ($ApoE^{-/-}$) were given a unilateral patellar tendon (PT) injury at 12 weeks old; the uninjured limb served as a control. Animals were euthanized at 3-, 14- or 42-days post-injury and PT healing was investigated. $ApoE^{-/-}$ serum cholesterol was double that of SD rats (mean 2.12 vs 0.99 mg/ml, p<0.001) and cholesterol level was related to the expression of several genes after injury; notably rats with higher cholesterol demonstrated a blunted inflammatory response. There was little physical evidence of tendon lipid content or differences in injury repair between groups, therefore we were not surprised that tendon mechanical or material properties did not differ between strains. The young age and the mild phenotype of our $ApoE^{-/-}$ rats might explain these findings. Hydroxyproline content was positively related to total blood cholesterol, but this result did not translate to observable biomechanical differences, perhaps due to the narrow range of cholesterol levels observed.

Tendon inflammatory and healing activity is modulated at the mRNA level even with a mild hypercholesterolemia. These important initial impacts need to be investigated as they may contribute to the known consequences of cholesterol on tendons in humans.

INTRODUCTION

Hypercholesterolemia is a condition characterized by elevated blood cholesterol levels. Once a distinct feature of high-income western countries, acquired high cholesterol is rising in low- and middle-income countries with changes in diet[1]. Hypercholesterolemia

can also be genetically inherited (familial) and as prevalent as $1/100^2$. Excess blood cholesterol is a major risk factor for developing cardiovascular disease due to its role in atherosclerosis and is associated with other preventable, age-related diseases (e.g. dementia[3]) as well as tendon ruptures[4; 5] and tendinopathies[6].

Xanthomas – lesions containing lipid-laden macrophages (or "foam cells") - are a physical manifestation of hypercholesterolemia commonly found under the skin and around superficial tendons[7]. Lipid accumulation among collagen fibers and fascicles may disrupt collagen organization within tendon and negatively affect its mechanical properties[8; 9]. There is evidence of this type of structure-function relationship in tendinosis[10] and tendinopathy[11], where expansion of the non-collagenous matrix from elevated proteoglycan content results in reduced stiffness and elastic storage potential, and increased hysteresis. Sub-clinical xanthomas are found in degenerative tendons, particularly with advancing age[12].

The pathophysiological mechanisms underpinning cholesterol deposition in tendons are not well characterised but are hypothesised to be similar to atherosclerosis[13]. Despite the prevalence of acute and chronic tendon injuries, there has been little research into the mechanisms by which cholesterol weakens tendon, hence their underlying aetiology often goes unexplained[14]. Recently, Steplewski et al.[15] discovered that high cholesterol weakens tendons via an unknown mechanism that causes physical damage to collagen fibrils. Hypercholesterolemia may impair tendon healing after an acute injury[16; 17], perhaps from lipid infiltration changing the mechanosensitive environment of tendon cell populations. Tendon cholesterol may therefore reduce an already slow and poor healing response to injury and subsequently increase the risk of progressive pathology.

We aim to ascertain the influence of hypercholesterolemia on tendon injury and repair using an established rat knock-out model to mimic familial hypercholesterolemia. This model results in defects in Apolipoprotein E (ApoE) - a critical protein used for transporting lipoproteins, fat-soluble vitamins, and cholesterol around the body - and brings about mild-moderate hypercholesterolemia without feeding a high-fat diet[18]. We will compare cell and tissue mechanobiology in this KO model with wild-type controls to explore the hypotheses that tendons exposed to chronically elevated levels of serum cholesterol will exhibit (a) greater localized levels of cholesterol accumulation, (b) abnormal mechanical properties, and (c) a hampered repair response to injury. The patellar tendon was chosen for investigation due to its loading-bearing function, superficial location and established injury model[19]. It also has a simple form for biomechanical testing and has previously shown evidence of lipid accumulation[8; 20]. The information obtained from our studies is of relevance because tendon disorders and injuries are widespread[21], cause significant pain and disability, and are notoriously complex to fully rehabilitate. Further, an association between cholesterol levels and tendon health is a particular concern, in light of the vicious cycle in which poor mobility and pain[22; 23] restricts exercise opportunities for patients, furthering the risk of elevated cholesterol[24]. Our findings will help to substantiate the mechanisms linking cholesterol levels and tendon injury risk, and the consequences of tendon cholesterol on tendon healing.

METHODS

Animal breeding and experimental procedures were approved by the local Animal Care Committee at the University of British Columbia (protocols #A17-0033 and A16-0256, respectively), and were carried out in accordance with the principles and standards of the

Canadian Council on Animal Care. The ARRIVE 2.0 checklist was consulted for transparent and accurate reporting[25].

Experimental Animals

We used young *ApoE*^{-/-} rats (SD- *ApoE* [tm1sage]; Horizon Discovery, Saint Louis, MO, USA), which demonstrate significantly elevated blood lipid profiles without feeding a high fat diet, to examine the effect of high cholesterol on tendon injury and repair processes. Whilst severity of hypercholesterolemia can be increased with feeding a high-fat diet, we wanted to avoid any comorbidities associated with it. Moreover, there is an associated increase in unexpected mortality and significantly reduced lifespan in these animals and so is not recommended[18]. Sprague-Dawley wild-type rats (SD; Charles River Laboratories, Wilmington, MA, USA) were used as control animals. Breeding pairs were co-housed when animals were 24 and 14 weeks, respectively. Rat husbandry was carried out by certified animal laboratory technicians. Rats were maintained on a 24-hr light/dark cycle between 21-24°C. All rats were fed regular chow (5% fat; PicoLab Rodent Diet 20: 5053, LabDiet; Richmond, IN, USA) for the study duration. Cages contained nesting material and environmental enrichment (plastic tubes, chew toys). Litters were weaned and sexed at 21 days old and sorted into group housing (2-3 per cage) located in a room separate from the breeders. Allocation to a post-injury group was completed on a cage-by-cage basis to help balance the male/female ratio at each time-point, and based on surgical suite and researcher scheduling logistics.

We investigated different aspects of tendon healing after injury at 3- 14- and 42- days post injury. These timepoints were chosen to target inflammatory, repair and remodelling processes, respectively. We determined that 20 animals per strain (tissue histology, n=6; gene expression, n=4; biomechanics, n=10) would allow a reasonable investigation of

each timepoint. However, only 50 $ApoE^{-/-}$ rats were successfully bred in total (50 SD rats were bred to match) and we omitted the 3-day post-injury timepoint from biomechanical testing, it being the least relevant to our hypotheses. All animals were used in this study; no inclusion or exclusion criteria were established. Equal male/female ratios were used where possible (total SD M23/F27, $ApoE^{-/-}$ M23/F27).

Surgical Protocol

All rats underwent a unilateral patellar tendon (PT) injury surgery at 12 weeks of age; the uninjured limb served as a control. Following UBC standard operating procedures, rats were anesthetized with a mixture of isoflurane (2-3%) and oxygen (100%) delivered via nose cone, and injected with warmed fluids (sterile lactated ringer's solution) and a pre-emptive dose of buprenorphine subcutaneously. Animals' ears were notched for identification, the incision area was prepared for surgery and a local analgesic delivered (by RM) to the incision site (Bupivacaine 0.25%, 4-8mg/kg subcutaneous). Rats were kept warm during the procedure via a warming pad.

Surgery was conducted aseptically; a 1-cm long incision was made on the medial side of the right knee and lateral displacement of the skin exposed the PT. An iris spatula was inserted behind the PT to provide a backing for a full thickness partial transection to the centre of the PT with a 0.75 mm diameter biopsy punch. Skin wounds were closed with subcuticular sutures and surgical glue. Animals resumed full mobility on regaining consciousness and were allowed to continue normal cage activity until they were sacrificed. Rats were monitored post-surgically and additional doses of analgesic given where necessary. >4% of animals required follow-up sutures after removing their original sutures; these animals were temporarily fitted with an Elizabethan collar. There were no additional complications post-surgery.

Tissue Harvesting

Rats were anaesthetized with a mixture of isoflurane (2-3%) and oxygen (100%) delivered via nose cone. 0.5ml of blood was collected in a lithium heparin tube via cardiac puncture just prior to euthanization with carbon dioxide, with death assured by cervical dislocation. Tendon tissues were harvested immediately thereafter.

Blood lipids

Immediately after collection, blood samples were centrifuged for 10 minutes at 2000g to separate plasma, and plasma samples stored at -80°C. Total blood serum cholesterol (free cholesterol and cholesteryl esters) was assessed with a fluorometric cholesterol assay (Invitrogen, cat. no. A12216).

qPCR

PT tissue was dissected from between the tibial tuberosity and patella with a sterile blade, taking care to remove the surrounding connective tissues and posterior fat pad, and stored short-term at -80°C. For RNA extraction, tendons were powdered in a tissue mill (Mikrodismembrator S, Sartorius, Germany) for 30s at 3,000 RPM in cryogenic tubes and suspended in 1ml Trizol. 0.2ml chloroform was then mixed with the homogenate and centrifuged at 12,000xg for 15 min at 4°C. The aqueous (top) phase was then transferred to an RNase-free tube and mixed with an equal volume of 100% ethanol.

RNA was purified using RNEasy columns according to the manufacturer's instructions (Qiagen, Mississauga, Canada). Quantitative PCR was performed using 7500 Fast Real-Time PCR System (Applied Biosystems, USA) and Luna® Universal One-Step RT-qPCR kit (E3005, New England Biolabs, Ipswich, MA, USA) according to the manufacturer's instructions. All samples were run in technical duplicate (cycle threshold

(Ct) s.d. = 0.34 cycles). The Ct mean of each target gene was normalized to that of

GAPDH and the uninjured PT of SD rats in the 42-day post-injury group were used as the

control. Primer sequences were designed and tested using NCBI/Primer-BLAST and

GeneRunner (v.3.05) or obtained from the literature[26] and synthesized by Applied

Biosystems Corp. (Foster City, California, United States; Table 1).

Histology

PT tissue was harvested as described for qPCR and embedded in OCT with the

orientation noted. Samples were flash frozen on a liquid nitrogen-cooled metal block and

kept at -80°C until required. Frozen tissue was sectioned on a cryostat at -22°C at 10μm

thicknesses in either the frontal or sagittal plane. Serial sections were acquired from the

mid-region of each sample and recovered onto adhesive coated slides (CryoJane, Leica

Microsystems Inc. Buffalo Grove, IL, USA). H&E staining was used to assess the general

structure, Oil Red-O staining for evaluating tissue lipid content, and IHC for examining

macrophage phenotypes. Perl's Prussian blue was used as a global stain for iron-

containing macrophages and counter-stained with nuclear fast red or Safranin-O.

Toludine blue was used to visualize mast cells.

Immunohistochemistry

Macrophage subpopulations were differentiated by staining for CD11b (M1 phenotype[27])

and CD206 markers (M2 phenotype[28]). Tissue sections were fixed in 95% ethanol,

washed for 5 minutes in tap water and incubated with 3% H_2O_2 at room temperature for 1

hr to quench endogenous peroxidase activity. Non-specific binding was blocked with

2.5% horse serum, followed by overnight incubation with primary antibodies at 4°C

(Table 2). Sections were washed in buffer and incubated with HRP Horse Anti-Mouse

IgG/AP Horse Anti-Rabbit IgG secondary antibodies for 10 minutes at room temperature,
followed by DAB and AP staining as per the manufacturer's instructions (ImmPRESS
duet double staining kit, cat no. MP-7724, Vector laboratories, UK). Spleen and lymph
node tissues were used as positive controls; isotype-matched IgG was used as a negative
control.

Biomechanics

The tibia-PT-patella complex of both legs were harvested, wrapped in PBS-soaked gauze
and stored at -20°C until required. Upon thawing, all soft tissue was dissected away from
the tibia and fibula, which was then set in dental stone (GC Fujirock Type IV Die Stone,
GC Corporation, Tokyo, Japan) until cured during which the PT was kept hydrated in
gauze. Tendon samples were scanned using high resolution micro-computed tomography
(40μm isotropic voxel size; Scanco uCT35, Scanco Medical AG, Brüttisellen,
Switzerland) for obtaining cross-sectional area (CSA). The potted sample was pinned to
an air-filter foam block for image contrast and to remove tendon slack, and encapsulated
in moistened gauze to prevent it from drying out. Tendon CSA was manually identified
from each transverse scan in the scanning software; the smallest CSA measured was used
in subsequent calculations (Fig. 1).

*** Figure 1 ***

After scanning, each sample was fixed within a material testing device (ElectroForce
5100, Bose Corporation, Eden Prairie, MN, USA) fitted with a 225N load cell. Tissue
clamps were lined with sandpaper to minimize the possibility of slippage. Samples were
pre-loaded to 1 N and tendon length measured using digital calipers. Specimens were
then sinusoidally loaded between 1 N and 15 N at 2 Hz for 30 cycles. For each loading-

unloading cycle, stress was determined by normalizing peak force to the PT CSA. Strain was calculated from peak extension normalized to sample preloaded length. Hysteresis was calculated as the area between the loading and unloading curves. Stiffness and modulus were estimated from the gradients of the force-extension and stress-strain curves respectively, using a linear regression model fitted between 50-90% of the loading curves (mean R^2 0.997±0.002). Mechanical properties were averaged for the last 10 cycles. Coefficients of variation (CV) were calculated over the last 10 cycles to confirm cycle consistency (strain, stiffness, hysteresis and force had CVs of 1.5, 1.7, 4.1 and 0.1%, respectively). The cyclic loading protocol was followed by a ramp-to-failure test, performed at 0.5 mm/s from which ultimate tensile (UT) strength and stress were determined. Load and displacement data for all tests were sampled at 200 Hz.

Hydroxyproline content

PTs used for biomechanical tests (42-day timepoint only) were dissected away from their remaining attachments and used to assess hydroxyproline content. 10 N NaOH was added to the tissue and heated to 100-120° overnight. Samples were cooled on ice and the hydrolysate neutralized by adding an equivalent volume of 10 N HCl; samples were vortexed, centrifuged at 10,000 x g for 5 minutes to pellet any insoluble debris and supernatant collected. 30 μl of each sample hydrolysate was transferred to a flat-bottom 96-well plate alongside a serial dilution of collagen type I solution with known concentration. 62.5 μl of oxidation reagent[29] was added to each well and the plate incubated at room temperature for 20 min. 62.5 μL of Ehrlich's solution was added to each well and the plate put on a shaker to mix. The plate was covered in aluminum foil and incubated at 65°C for 30 min; chromophore development was stopped by putting the

plate on ice and the plate read in a spectrophotometer at an absorbance wavelength of 560 nm.

Statistics

Experiments were blinded, since ear notch identification (used for tissue identification) was completed in no particular sequence. Once data was processed, ear notch ID was matched to rat ID (strain, timepoint) for analyses. Statistical analysis was done using SPSS statistical software (v23, IBM Corp., Armonk, NY, USA). Blood cholesterol levels and weights were compared between rat strains with independent t-tests. Analysis of qPCR data were completed on $2^{-\Delta\Delta CT}$ values with one-way ANOVA to examine 1) between-group differences relative to the control group, and 2) within group timepoints. To assess the biomechanical properties of non-injured PT between groups, an initial MANCOVA (sex as covariate) was used. Biomechanical properties at 14- and 42-days post injury were examined with separate MANCOVAs (Leg side x group; sex as covariate). Hydroxyproline assay results were analysed by one-way ANOVA and Tukey's multiple comparison test. Correlations between total cholesterol level (independent of group) and all dependent variables were also assessed with regression analyses. Given the mild *ApoE*$^{-/-}$ phenotype, sample sizes may be underpowered for some statistical tests.

RESULTS

Cholesterol/weight/macroscopic diffs

Mean animal age on injury date was 12.2±0.8 weeks. Male rats were heavier than female rats. SD males were heavier than *ApoE*$^{-/-}$ males at injury date (mean 394.0g vs. 363.7g, p=0.009); weights of SD and *ApoE*$^{-/-}$ female rats did not differ (mean 254.3g vs. 241.2g,

p=0.421). *ApoE*$^{-/-}$ total cholesterol (TC) was over double that of SD rats (mean 2.12 vs. 0.99 mg/ml, Fig. 2) with some overlap between groups. There were no sex differences in TC within each strain and no obvious macroscopic differences in tissue appearance between groups.

*** Figure 2 ***

Histology

There were no apparent histological differences in the PT of *ApoE*$^{-/-}$ vs SD rats, either in injured or uninjured tendons. Areas of injury were easily identified by increased cellularity, disrupted fibril alignment and deposition of ground substance (Fig. 3). The injury site became less obvious with timepoint progression although there were notable histological differences between injuries. Close inspection of the histology indicated that these differences likely arose from the surgical procedure. In some instances, the biopsy punch fully removed the tissue (hereafter termed 'large injury') whilst in others, the tissue remained in place afterwards (hereafter termed 'small injury'). An example is shown in Fig. 3. An analysis of the histology indicated that ~53% (19/36) of the samples were large injuries, however it is not possible to determine which injury type the samples undergoing mechanical characterisation or PCR analysis received.

The PT of both strains of rats showed very little positive lipid staining with Oil Red-O with no observable differences between groups or timepoints.

*** Figure 3 ***

CD11b and CD206 markers were identified in small numbers and not in all sections; staining was inconsistent with no obvious correlation to group or timepoint (Fig. 3).

Immune cells were present in uninjured and injured tissue. In uninjured tissue and sections with small injuries, macrophages and mast cells were largely restricted to the peritendon. In sections demonstrating large injuries, mast cells and macrophages were also seen at the injury site, however the high density of cell nuclei at injury sites were cells other than immune cells (Fig. 3).

qPCR

As expected, inflammatory markers COX2 and IL1 were more highly expressed in early injury repair. LOX expression increased after injury and remained elevated throughout the healing process. In line with previous reports, e.g. [30], COL1A1 and COL3A1 expression peaked at 14 days post-injury in both groups. The pattern of gene expression over the injury repair time course did not differ considerably between SD and $ApoE^{-/-}$ rats (Fig. 4A). However, differences in gene expression were seen with cholesterol level when groups were combined by time point (Fig. 4B). The inflammatory response (COX-2, IL-1) was positively correlated with serum cholesterol level at 3 days post-injury. COL1A1 expression was also correlated with serum cholesterol level at 42 days post-injury. All other genes and timepoints were statistically unrelated to cholesterol level.

*** *Figure 4* ***

Tissue Biomechanics

71 specimens (36 animals) were successfully analysed for biomechanical properties. Biomechanical testing was performed for the 14- and 42-day timepoints. Technical issues in dissecting the patella-PT-tibia complex resulted in only 6 $ApoE^{-/-}$ rat specimens at the 14-day timepoint. Of the samples tested, 32/71 of PT specimens failed at the patellar insertion, 27/71 failed at the tibial insertion and 15/71 pulled out of clamp/mould during

the ramp-to-failure test prior to failure. Specimens that slipped during the failure test were not included in the ramp-to-failure analyses, leading to smaller sample sizes for properties estimated from these tests (Fig. 5). They were retained in the initial cyclic analysis, where data demonstrated that slippage had not occurred until higher loads were applied. There was no relation between failure mode and experimental grouping.

For non-injured PTs, multivariate tests found timepoint was insignificant, hence the 14- and 42-day timepoints were combined. A MANCOVA found sex trended as a co-variate (p=0.063). Follow-up tests found CSA and cyclic peak stress was significantly affected by sex (p=0.001); female rats had smaller PT CSA and therefore larger stress values at the same force values. No other biomechanical differences were found between groups. In the 14- and 42-day MANCOVAs, no differences between groups or limbs were found in the mechanical or material properties evaluated with either cyclic or failure tests, nor were any differences identified in PT gross morphology (preloaded tendon length, CSA; Fig. 5). Regression analysis of individual biomechanical properties found the UT strength of the non-injured side was positively correlated with cholesterol levels ($R^2 = 0.22$, p=0.015); no other biomechanical properties (injured or non-injured limb) were found to be significantly associated with total serum cholesterol.

*** *Figure 5* ***

Hydroxyproline content

Total hydroxyproline content did not differ significantly between comparable limbs of SD and *ApoE*$^{-/-}$ rats, or between the uninjured versus injured limbs of each group (Fig. 6A). However, hydroxyproline content was significantly, positively related to total serum cholesterol (Fig. 6B, p=0.011).

*** *Figures 6A, 6B* ***

DISCUSSION

In this study, we investigated the impact of elevated cholesterol levels on tendon healing after an acute injury. We found injury repair at the mRNA level was related to total cholesterol level rather than differing between the *ApoE*^{-/-} rat model and control animals. We did not find differences between rat strains in histology or biomechanical properties. Hydroxyproline content was significantly associated with cholesterol level but did not differ between strains. Our results indicate that mild hypercholesterolemia - rather than rat strain - may impact healing processes but does not significantly impact tendon strength.

The *ApoE*^{-/-} rats in this study showed elevated blood cholesterol levels compared to SD control rats, but only to about half of that predicted[18]. This resulted in some overlap in cholesterol levels between the *ApoE*^{-/-} the SD group. A high fat diet would have enhanced the lipid profiles of these animals in the present study[31; 32] but at the expense of higher mortality rates and reduced lifespan[18; 32], hence it is not recommended by the supplier.

The relative absence of lipid staining in our histological sections suggests that physical accumulation of lipids in the PT is minimal in *ApoE*^{-/-} rats, confirming the mild phenotype. Due to these initial findings we found we could not test the hypothesis that tendons exposed to chronically elevated levels of serum cholesterol would be associated with greater localized levels of cholesterol accumulation. Although lipids and xanthomas have been previously detected in the PT, staining might have been evident in tendons

where the interfascicular matrix and vasculature is more extensive, such as the Achilles or flexor digitorum[33; 34]. This hypothesis should be revisited with an appropriate model.

We examined immune cell populations in injured and non-injured tendon tissue due to reports of macrophage polarization in injury repair, atherosclerotic plaque and xanthoma development[35; 36]. CD11b is considered a total macrophage marker[37] and CD206 is,useful for differentiating the pro-healing M2 macrophages[38]. While both markers were identified with IHC, the lack of consistency across timepoints and strains, coupled with unintentionally creating two injury types, makes it impossible to draw conclusions from this finding. Other histochemical methods gave us a sense of total immune cell numbers (which were surprisingly low, even in large injuries) and locations, but examining immune cells in tendons with confirmed intratendinous lipids should be done in future to better gauge their associations with cholesterol levels.

We hypothesised that intratendinous lipid accumulation would alter the tenocyte's local environment and negatively affect the $ApoE^{-/-}$ cellular repair profile, but found no difference in the magnitude or time-course of gene expression compared to SD rats (Fig. 4A). This is likely due to low statistical power and significant within-group data variability. When combining groups by timepoint (which increased our statistical power) we found the expression of inflammatory markers COX-2 and IL1 were significantly correlated with cholesterol levels in early injury repair, such that the inflammatory response was reduced as cholesterol increased (Fig. 4B). Acute inflammation is essential for tendon healing thus a diminished inflammatory response with elevated cholesterol might translate to impaired tissue healing[39]. Although we did not detect impaired healing via histological or biomechanical investigations, the small injury size relative to tendon

size may have been insufficient to warrant detectable phenotypic differences resulting from the observed alterations in gene expression.

LOX plays a significant role in tissue repair and remodelling processes, namely by catalyzing the cross-linking of ECM components for tissue stability[40]. Both LDL[41] and oxLDL[42] have been shown to downregulate LOX expression, which led us to hypothesize that LOX expression would be reduced with elevated cholesterol, but this wasn't the case. Perhaps LDL or oxLDL levels presently were low enough to not impact LOX expression in the healing PT. COL1A1, but not COL3A1, appeared suppressed in the later stages of healing with elevated cholesterol. COL1A1 encodes the alpha 1 chain of type I collagen – the molecule that provides tendons with their tensile strength and replaces weaker collagen types in the remodelling process. The negative relationship with cholesterol may indicate a slower transition to mature tissue with mild hypercholesterolemia.

Hydroxyproline (3-hyp, 4-hyp) was used as a surrogate measure of collagen in PT tissue. Injured tendons generally demonstrated a (non-significantly) lower hydroxyproline content than uninjured tendon, perhaps reflecting a loss of collagen, increased cellularity, or increased ground substance with trauma. *ApoE$^{-/-}$* rats generally had a higher hydroxyproline content than SD animals, and a more detailed examination of this association led to finding a positive correlation with cholesterol level. As hydroxyproline assays do not differentiate between collagen type, and hydroxyproline content is higher in the weaker type III collagen (UniProt: collagen I, 223x4-hyp, 10x3-hyp; collagen III, 435x4-hyp, 0x3-hyp[43; 44]), a higher hydroxyproline content could also indicate a higher collagen III content. Supporting this idea, a 4-fold increase in the ratio of collagen III to collagen I was recently found in the tendons of high cholesterol rabbits[15].

There are several factors that should be considered when explaining our biomechanical findings. The biopsy punch injury is an accepted and reproducible model for studying basic mechanisms of tendon repair[19], however the 0.75mm punch size in relation to the PT width of our rats was perhaps too small to affect tendon biomechanics. Moreover, discovering that the biopsy had not always removed tissue and so created two distinct injury types may have made it more difficult to identify differences between strains. However, variability seems to be comparable between injured and non-injured tendons, indicating that the different injuries might not cause a higher variation. Other injury/repair models such as a window defect, partial or full transection [45-47] may have delivered a more pronounced affect on tendon biomechanics. However, our chosen method did not require suture repair, which might add to or alter the normal biological processes at the injury site (e.g., increased inflammation), nor did it result in unloading from animals avoiding weightbearing on the injured limb. This is particularly important as mechanical loading has been shown to accelerate tendon healing and recovery[48]. We also had a lower-than-expected sample size for biomechanical investigations, which should be considered when interpreting the statistical results of this experiment. Nonetheless, results are generally in agreement with other studies using young $ApoE^{-/-}$ rodent models in finding few differences in PT biomechanical properties compared to wild-type controls [8; 49].

Young $ApoE^{-/-}$ rats fed a regular diet produced a mild hypercholesterolemia model in our study. Older animals with higher plasma cholesterol[50] and/or a longer exposure to high cholesterol levels[49] may have provided a more moderate hypercholesterolemia model. Certainly other hyperlipidemic models demonstrate moderate or severe phenotypes and

evidence of tendon lipid deposits to better reflect FH in humans[34; 51; 52]. With the availability of genome editing techniques, models of hyperlipidemia for generalizing research results from animals to humans[53] should be taken advantage of in future research.

CONCLUSION

We found elevated blood cholesterol levels were related to the expression of injury repair genes and may negatively affect tendon repair after injury. Although there was little evidence of lipid accumulation at the tissue level, perhaps due to our young rat cohorts, there was a significant relationship between total blood cholesterol and PT hydroxyproline content. Our results substantiate the link between cholesterol level and tendon injury risk and indicate that even mildly elevated cholesterol levels can modulate tendon inflammatory and healing activity. These impacts need further investigation as they may contribute to the known consequences of cholesterol on tendons in humans.

DISCLOSURES

The authors have no conflicts of interest to report.

REFERENCES

1. Collaboration NCDRF. 2020. Repositioning of the global epicentre of non-optimal cholesterol. Nature 582:73-77.
2. Hu P, Dharmayat KI, Stevens CAT, et al. 2020. Prevalence of Familial Hypercholesterolemia Among the General Population and Patients With Atherosclerotic Cardiovascular Disease: A Systematic Review and Meta-Analysis. Circulation 141:1742-1759.
3. Meng XF, Yu JT, Wang HF, et al. 2014. Midlife vascular risk factors and the risk of Alzheimer's disease: a systematic review and meta-analysis. Journal of Alzheimer's disease: JAD 42:1295-1310.
4. Abboud JA, Kim JS. 2010. The effect of hypercholesterolemia on rotator cuff disease. Clin Orthop Relat Res 468:1493-1497.
5. Ozgurtas T, Yildiz C, Serdar M, et al. 2003. Is high concentration of serum lipids a risk factor for Achilles tendon rupture? Clin Chim Acta 331:25-28.
6. Klemp P, Halland AM, Majoos FL, et al. 1993. Musculoskeletal manifestations in hyperlipidaemia: a controlled study. Ann Rheum Dis 52:44-48.
7. Bude RO, Adler RS, Bassett DR. 1994. Diagnosis of Achilles tendon xanthoma in patients with heterozygous familial hypercholesterolemia: MR vs sonography. AJR American journal of roentgenology 162:913-917.
8. Grewal N, Thornton GM, Behzad H, et al. 2014. Accumulation of oxidized LDL in the tendon tissues of C57BL/6 or apolipoprotein E knock-out mice that consume a high fat diet: potential impact on tendon health. PloS one 9:e114214.
9. Squier K, Scott A, Hunt MA, et al. 2021. The effects of cholesterol accumulation on Achilles tendon biomechanics: A cross-sectional study. PloS one 16:e0257269.
10. Khan KM, Bonar F, Desmond PM, et al. 1996. Patellar tendinosis (jumper's knee): findings at histopathologic examination, US, and MR imaging. Victorian Institute of Sport Tendon Study Group. Radiology 200:821-827.
11. Wang HK, Lin KH, Su SC, et al. 2012. Effects of tendon viscoelasticity in Achilles tendinosis on explosive performance and clinical severity in athletes. Scand J Med Sci Sports 22:e147-155.
12. Józsa LG, Kannus P. 1997. Human tendons: anatomy, physiology, and pathology. Champaign, IL: Human Kinetics;
13. Oosterveer DM, Versmissen J, Yazdanpanah M, et al. 2010. The risk of tendon xanthomas in familial hypercholesterolaemia is influenced by variation in genes of the reverse cholesterol transport pathway and the low-density lipoprotein oxidation pathway. Eur Heart J 31:1007-1012.
14. Soslowsky LJ, Fryhofer GW. 2016. Tendon Homeostasis in Hypercholesterolemia. Adv Exp Med Biol 920:151-165.
15. Steplewski A, Fertala J, Tomlinson R, et al. 2019. The impact of cholesterol deposits on the fibrillar architecture of the Achilles tendon in a rabbit model of hypercholesterolemia. J Orthop Surg Res 14:172.
16. Beason DP, Tucker JJ, Lee CS, et al. 2014. Rat rotator cuff tendon-to-bone healing properties are adversely affected by hypercholesterolemia. J Shoulder Elbow Surg 23:867-872.

17. Chung SW, Park H, Kwon J, et al. 2016. Effect of Hypercholesterolemia on Fatty Infiltration and Quality of Tendon-to-Bone Healing in a Rabbit Model of a Chronic Rotator Cuff Tear: Electrophysiological, Biomechanical, and Histological Analyses. Am J Sports Med 44:1153-1164.

18. Smidt N, van der Windt DA, Assendelft WJ, et al. 2002. Interobserver reproducibility of the assessment of severity of complaints, grip strength, and pressure pain threshold in patients with lateral epicondylitis. Arch Phys Med Rehabil 83:1145-1150.

19. Lin TW, Cardenas L, Glaser DL, et al. 2006. Tendon healing in interleukin-4 and interleukin-6 knockout mice. Journal of biomechanics 39:61-69.

20. Kannus P, Jozsa L. 1991. Histopathological changes preceding spontaneous rupture of a tendon. A controlled study of 891 patients. The Journal of bone and joint surgery American volume 73:1507-1525.

21. Gaida JE, Alfredson H, Kiss ZS, et al. 2010. Asymptomatic Achilles tendon pathology is associated with a central fat distribution in men and a peripheral fat distribution in women: a cross sectional study of 298 individuals. BMC Musculoskelet Disord 11:41.

22. Beeharry D, Coupe B, Benbow EW, et al. 2006. Familial hypercholesterolaemia commonly presents with Achilles tenosynovitis. Ann Rheum Dis 65:312-315.

23. Rechardt M, Shiri R, Lindholm H, et al. 2013. Associations of metabolic factors and adipokines with pain in incipient upper extremity soft tissue disorders: a cross-sectional study. BMJ Open 3:e003036.

24. Mann S, Beedie C, Jimenez A. 2014. Differential effects of aerobic exercise, resistance training and combined exercise modalities on cholesterol and the lipid profile: review, synthesis and recommendations. Sports Med 44:211-221.

25. Percie du Sert N, Ahluwalia A, Alam S, et al. 2020. Reporting animal research: Explanation and elaboration for the ARRIVE guidelines 2.0. PLoS Biol 18:e3000411.

26. Heinemeier KM, Olesen JL, Schjerling P, et al. 2007. Short-term strength training and the expression of myostatin and IGF-I isoforms in rat muscle and tendon: differential effects of specific contraction types. J Appl Physiol (1985) 102:573-581.

27. Schmid MC, Khan SQ, Kaneda MM, et al. 2018. Integrin CD11b activation drives anti-tumor innate immunity. Nat Commun 9:5379.

28. Colin S, Chinetti-Gbaguidi G, Staels B. 2014. Macrophage phenotypes in atherosclerosis. Immunol Rev 262:153-166.

29. Cissell DD, Link JM, Hu JC, et al. 2017. A Modified Hydroxyproline Assay Based on Hydrochloric Acid in Ehrlich's Solution Accurately Measures Tissue Collagen Content. Tissue Eng Part C Methods 23:243-250.

30. Juneja SC, Schwarz EM, O'Keefe RJ, et al. 2013. Cellular and molecular factors in flexor tendon repair and adhesions: a histological and gene expression analysis. Connect Tissue Res 54:218-226.

31. Wei S, Zhang Y, Su L, et al. 2015. Apolipoprotein E-deficient rats develop atherosclerotic plaques in partially ligated carotid arteries. Atherosclerosis 243:589-592.

32. Rune I, Rolin B, Lykkesfeldt J, et al. 2018. Long-term Western diet fed apolipoprotein E-deficient rats exhibit only modest early atherosclerotic characteristics. Scientific reports 8:5416.

33. Lee AH, Elliott DM. 2019. Comparative multi-scale hierarchical structure of the tail, plantaris, and Achilles tendons in the rat. Journal of anatomy 234:252-262.

34. Nakano A, Kinoshita M, Okuda R, et al. 2006. Pathogenesis of tendinous xanthoma: histopathological study of the extremities of Watanabe heritable hyperlipidemic rabbits.

Journal of orthopaedic science: official journal of the Japanese Orthopaedic Association 11:75-80.

35. Mantovani A, Garlanda C, Locati M. 2009. Macrophage diversity and polarization in atherosclerosis: a question of balance. Arterioscler Thromb Vasc Biol 29:1419-1423.

36. Fadini GP, Simoni F, Cappellari R, et al. 2014. Pro-inflammatory monocyte-macrophage polarization imbalance in human hypercholesterolemia and atherosclerosis. Atherosclerosis 237:805-808.

37. Taylor PR, Martinez-Pomares L, Stacey M, et al. 2005. Macrophage receptors and immune recognition. Annu Rev Immunol 23:901-944.

38. Ezekowitz RA, Gordon S. 1984. Alterations of surface properties by macrophage activation: expression of receptors for Fc and mannose-terminal glycoproteins and differentiation antigens. Contemp Top Immunobiol 13:33-56.

39. Ghosh N, Kolade OO, Shontz E, et al. 2019. Nonsteroidal Anti-Inflammatory Drugs (NSAIDs) and Their Effect on Musculoskeletal Soft-Tissue Healing: A Scoping Review. JBJS Rev 7:e4.

40. Cai L, Xiong X, Kong X, et al. 2017. The Role of the Lysyl Oxidases in Tissue Repair and Remodeling: A Concise Review. Tissue Eng Regen Med 14:15-30.

41. Rodriguez C, Raposo B, Martinez-Gonzalez J, et al. 2002. Low density lipoproteins downregulate lysyl oxidase in vascular endothelial cells and the arterial wall. Arterioscler Thromb Vasc Biol 22:1409-1414.

42. Mousavizadeh R, DeBruin E, Waugh C, et al. oxLDL disrupts matrix remodelling and synthesis by human tendon cells. [unpublished work].

43. Kuivaniemi H, Tromp G. 2019. Type III collagen (COL3A1): Gene and protein structure, tissue distribution, and associated diseases. Gene 707:151-171.

44. Weis MA, Hudson DM, Kim L, et al. 2010. Location of 3-hydroxyproline residues in collagen types I, II, III, and V/XI implies a role in fibril supramolecular assembly. J Biol Chem 285:2580-2590.

45. Chan BP, Fu S, Qin L, et al. 2000. Effects of basic fibroblast growth factor (bFGF) on early stages of tendon healing: a rat patellar tendon model. Acta Orthop Scand 71:513-518.

46. Jiang D, Gao P, Lin H, et al. 2016. Curcumin improves tendon healing in rats: a histological, biochemical, and functional evaluation. Connect Tissue Res 57:20-27.

47. Uslu M, Kaya E, Yaykasli KO, et al. 2015. Erythropoietin stimulates patellar tendon healing in rats. Knee 22:461-468.

48. Khayyeri H, Hammerman M, Turunen MJ, et al. 2020. Diminishing effects of mechanical loading over time during rat Achilles tendon healing. PloS one 15:e0236681.

49. Beason DP, Abboud JA, Kuntz AF, et al. 2011. Cumulative effects of hypercholesterolemia on tendon biomechanics in a mouse model. Journal of orthopaedic research: official publication of the Orthopaedic Research Society 29:380-383.

50. Parini P, Angelin B, Rudling M. 1999. Cholesterol and lipoprotein metabolism in aging: reversal of hypercholesterolemia by growth hormone treatment in old rats. Arterioscler Thromb Vasc Biol 19:832-839.

51. Kaabia Z, Poirier J, Moughaizel M, et al. 2018. Plasma lipidomic analysis reveals strong similarities between lipid fingerprints in human, hamster and mouse compared to other animal species. Scientific reports 8:15893.

52. Watanabe Y. 1980. Serial inbreeding of rabbits with hereditary hyperlipidemia (WHHL-rabbit). Atherosclerosis 36:261-268.

53.   Zhao Y, Qu H, Wang Y, et al. 2020. Small rodent models of atherosclerosis. Biomed Pharmacother 129:110426.

Table 1. Oligonucleotide sequence of primers of selected rat genes

Target Gene	Forward Primer	Reverse Primer
COX-2	CCT TCC TCC TGT GGC TGA TGA C	ACA CCT CTC CAC CGA TGA CC
IL-1B	CCT TGC AGC TGG AGA GTG TGG AC	ACC AGT TGG GGA ACT GTG CAG
LOX AGT	CAG GCA CCG ACC TGG ATA TGG	CGT ACG TGG ATG CCT GGA TGT
COL1A1	ATC AGC CCA AAC CCC AAG GAG AG	CGC AGG AAG GTC AGC TGG ATA G
COL3A1 TT	TGA TGG GAT CCA ATG AGG GAG A	GAG TCT CAT GGC CTT GCG TGT

Table 2. Details of the primary antibodies used for immunohistochemical staining.

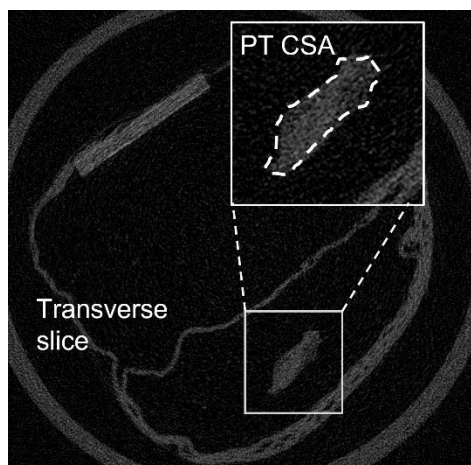| Antibody	Host Species	Mono/polyclonal	Concentration	Manufacturer; Product Code
Anti-Mannose Receptor (CD206)	Rabbit IgG	Polyclonal	1:400	Abcam; ab64693
CD11b	Mouse IgG	Monoclonal	1:100	Biorad; MCA275GA
Negative control	Mouse IgG2a		1:400	Biorad; MCA929
Negative control	Rabbit IgG		1:400	In-house preparation

Figure 1. Cross-sectional microCT images from which tendon CSA was obtained. Black image regions represent less dense material (e.g. air filter) whereas white regions represent more dense material (e.g. bone). Image contrast is relative to minimum and maximum pixel values.
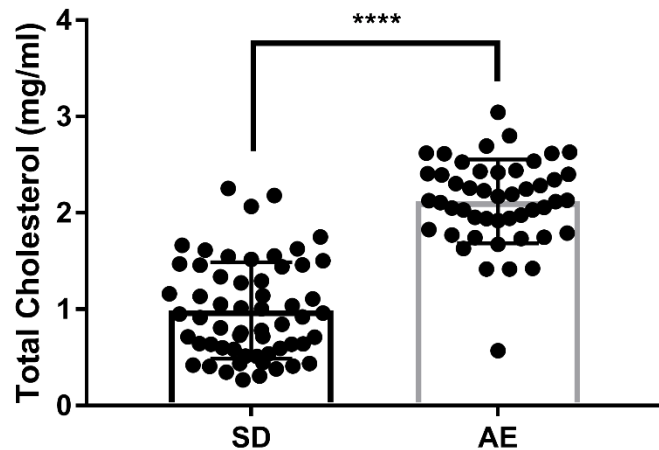

Figure 2. Serum cholesterol levels of ApoE$^{-/-}$ and SD rats were significantly different ****p<0.001
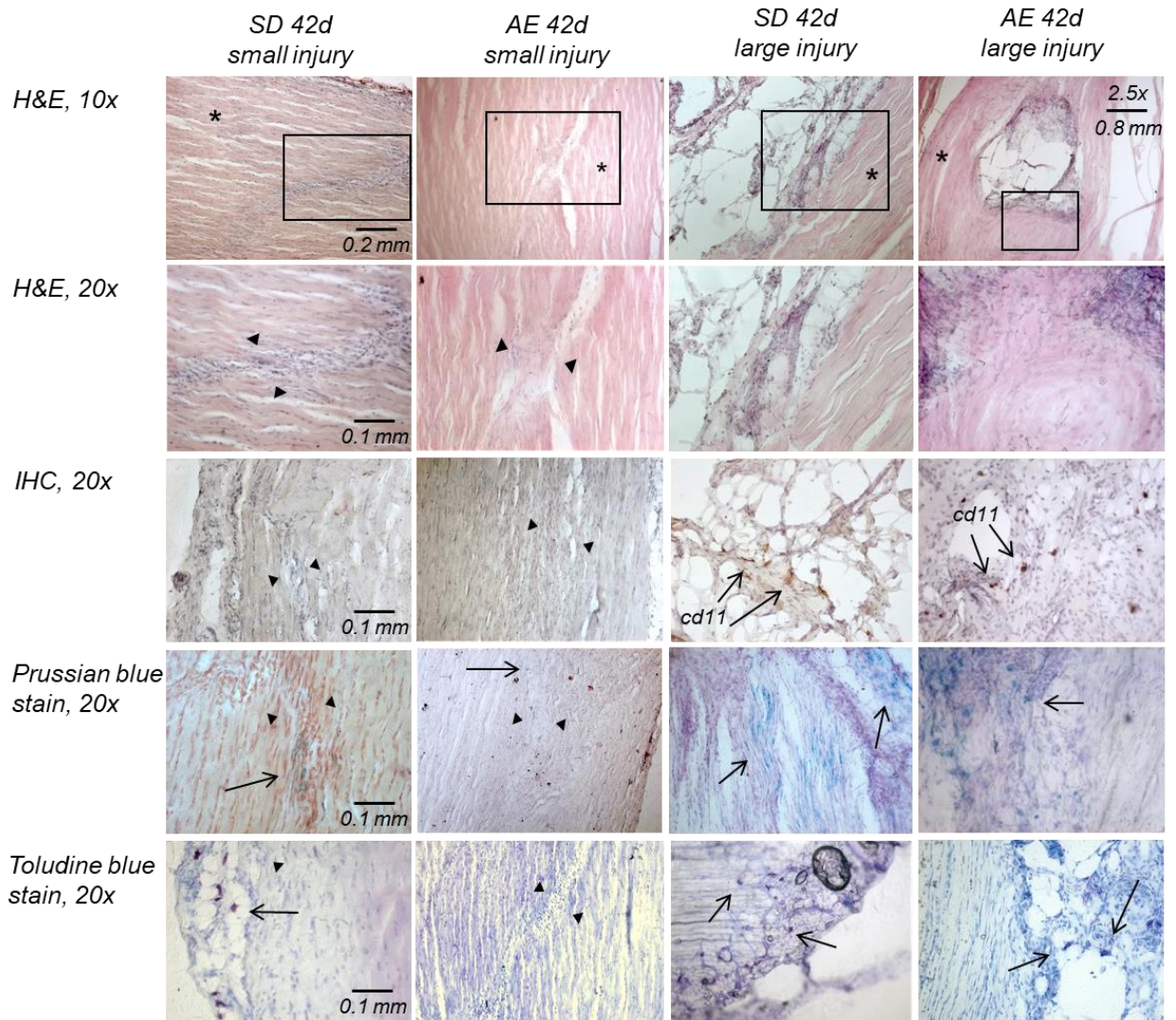
Figure 3. Histological evidence of small and large tissue injuries and immune cell locations. H&E staining demonstrates injury evidence, e.g. increased cellularity, discontinuation of collagen fibres and disorganized tissue; black boxes in H&E 10x images indicate injury area magnified in H&E 20x. Black wedges in small injury example (left column) highlight less obvious injury site. Asterisks indicate aligned collagen fibres in non-injured areas. IHC (polarized macrophages), Perl's Prussian blue (macrophages, blue) and toludine blue staining (mast cell granules, purple) help to identify immune cells

relative to injury site; arrows point to immune cell staining. Scale bar for magnification shown in left-hand images unless otherwise indicated.
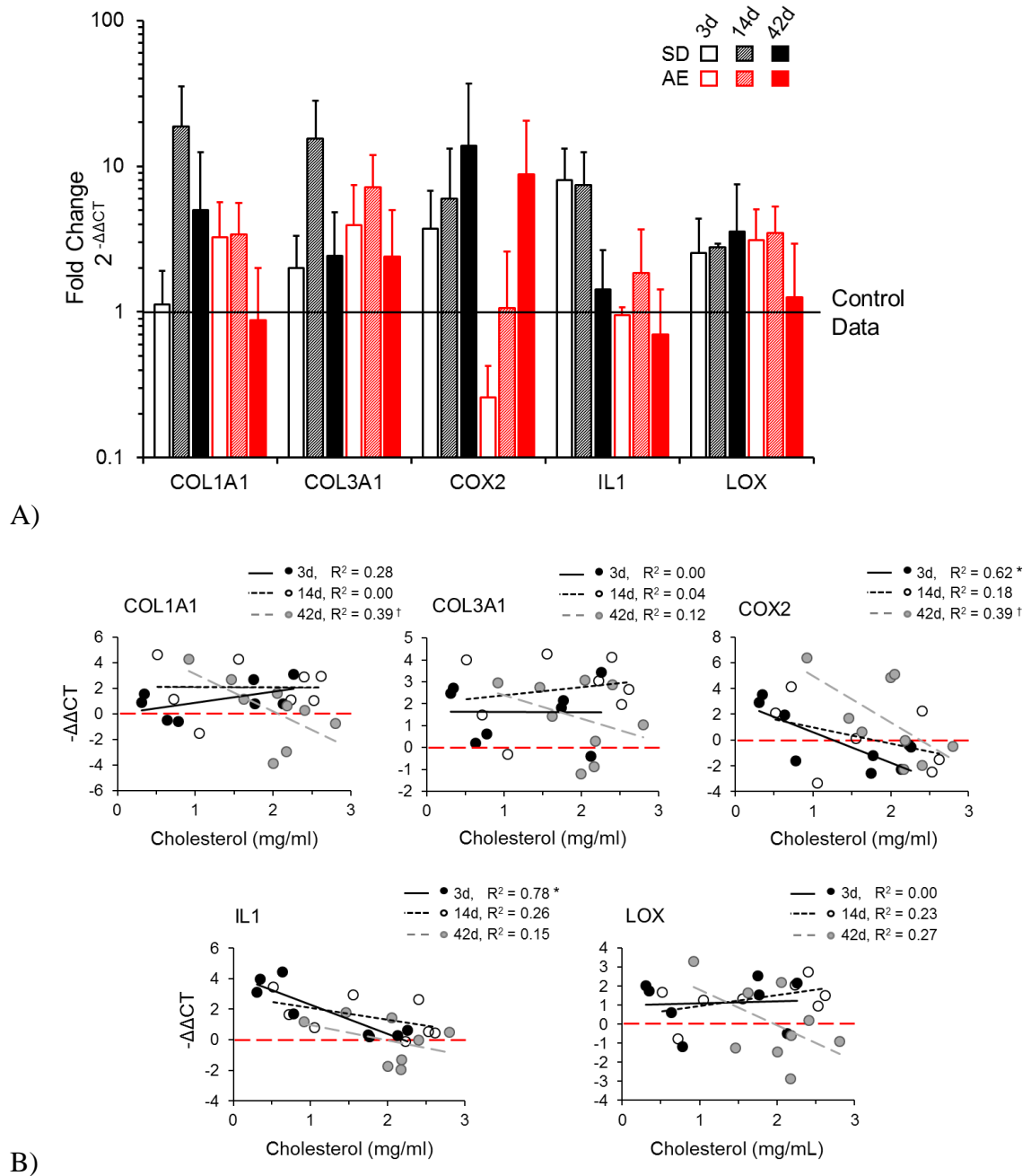

A)

B)

Figure 4. Quantitative PCR results showing A) pattern of gene expression after PT injury (n=4 per group/time-point), and B) relationship with serum cholesterol levels at each timepoint (SD and AE groups combined, n=8). All data are relative to control condition

(non-injured SD PT at 42 days post-injury) indicated by A) solid black line at y=1 and B) red dashed line at y=0. *p<0.05, †p<0.1.
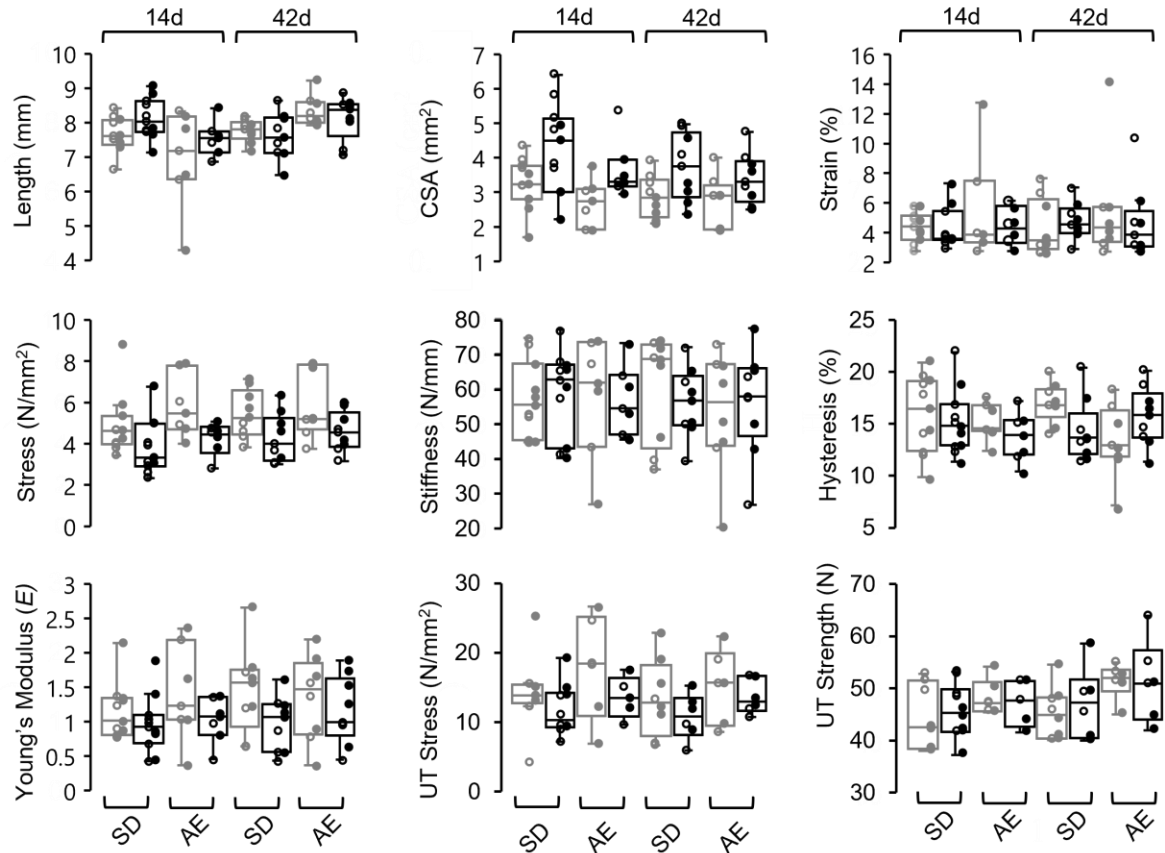

Figure 5: Boxplot of PT biomechanical properties showing data quartiles and median; outliers are not connected by whiskers. Individual data points are superimposed on bars; unfilled circles - male, filled circle - female. Black boxes represent injured (right, experimental) limb, grey boxes represent uninjured (left, control) limb. Data presented by group (SD, AE) and timepoint (14 days, 42 days). No differences between groups or timepoints were found in any variable examined.
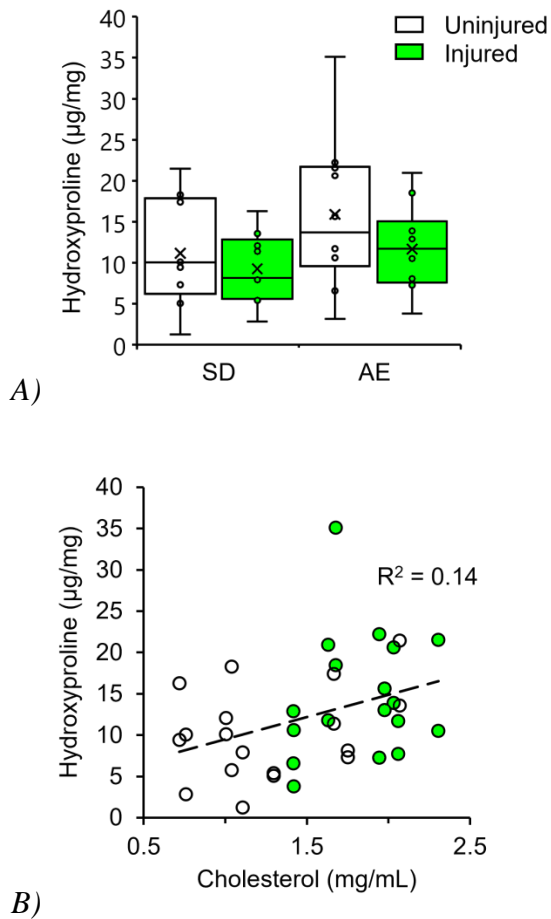
A)

B)

Figure 6. A) Hydroxyproline content in PT by group and limb, analysed with one way ANOVA. B) Relation between total blood cholesterol and hydroxyproline content. SD; open circles, ApoE$^{-/-}$; filled circles. L/R leg separate data points, p=0.011.